EurJIC
European Journal of Inorganic Chemistry

Research Article
doi.org/10.1002/ejic.202500126

Chemistry Europe
European Chemical Societies Publishing

www.eurjic.org

Structural and Kinetics Studies of N^O-, O^N^O-, and N^N- Schiff Base Mn Complexes as Highly Active Catalysts in the Ring-Opening Polymerization of *rac*-Lactides

Mnqobi Zikode, Asanda Ngwenya, Tabea Becker, Sonja Herres-Pawlis, and Stephen. O. Ojwach*

A series of manganese complexes derived from (imino)phenol/pyridine proligands have been synthesized, structurally characterized and used as catalysts in the ring-opening polymerization (ROP) of *rac*-lactides (*rac*-LA). Reactions of $MnCl_2{\cdot}4H_2O$ salt with 2-[((2-hydroxyethyl)imino)methyl]phenol (**L1H$_2$**) afford a tetranuclear Mn(III) complex [Mn(**L1**)Cl]$_4$ (**Mn1**). Separately, treatment of $MnCl_2{\cdot}4H_2O$ with 2-[((2-methoxyethyl)imino)methyl]phenol (**L2H**) gave the mononuclear Mn(II) complex [Mn(**L2**)$_2$(CH_3OH)$_2$] (**Mn2**). Further, reactions of (imino)pyridine proligands ((E)-2-((pyridine-2-ylmethylene)amino)ethan-1-ol (**L3H**) and (E)-N-(2-methoxyethyl)-1-(pyrid-2-yl)methanimine (**L4**)) with $MnCl_2{\cdot}4H_2O$ afforded polynuclear Mn(II) complexes [Mn(**L3H**)Cl$_2$]$_3$ (**Mn3**) and [Mn(**L4**)Cl$_2$]$_3$ (**Mn4**), respectively. The molecular structure of **Mn1** established the tridentate binding mode of the dianionic alkoxy-(imino)phenol proligand ((**L1**$^{2-}$)) through the phenoxo and pendant-arm alkoxy-oxygen and the imine-nitrogen atoms. In contrast, the molecular structure of **Mn2** showed that the ether-(imino)phenol pro-ligand (**L2H**) is monoanionic (**L2**$^-$) and bidentately coordinated to the Mn(II) metal center through the phenoxo-oxygen and the imine-nitrogen atoms. The dinuclear complex **Mn3** contains a neutral N^N bidentately bound proligand (**L3H**). All the complexes (**Mn1**–**Mn4**) formed active catalysts in ROP of *rac*-LA with the propagation rate constant k_p of up to $(4.25 \pm 0.15) \times 10^{-2}$ L mol^{-1} s^{-1}. The polymers obtained were atactic biased ($P_r = 0.55$–0.59), produced with moderate control over average-number molecular weights and were moderately dispersed ($Đ$ up to 1.8) under melt conditions.

1. Introduction

Approximately 70% of all conventional fossil-based plastics produced end up in landfills and consequently contribute to environmental pollution.[1,2] Recently, the global pandemic (COVID-19) clearly demonstrated how heavily the modern world depends on plastics in order to maintain modern societal life challenges.[3] For example, the plastic packaging material, syringes, and face masks used during the pandemic were made from plastics. Thus, a greater need to develop biobased plastics produced from naturally renewable resources has become even more indispensable.[4] Owing to their potential sustainability, environmental friendliness, and biological applicability, polylactides (PLAs) are considered commercially promising bioplastics and a green substitute to the fossil-based polymers.[5–8] Thus, PLA have found applications in various fields including agriculture,[9] biomedical,[10–20] electronics,[21] textile,[9,22,23] pharmaceutical, and packaging industries.[24–28]

While PLA is biodegradable and biocompatible,[29–38] its full potential has not been realized due to the use of toxic stannous octate (Sn(oct)$_2$) catalyst in its industrial production.[39] This has led to the resurgence of the design of alternative catalysts derived from benign metals, such as Fe(II),[40–42]] Zn(II),[43–53] and Mg.[54–60] Another promising metal which can be used to synthesise the ROP catalysts is manganese owing to its naturally abundance, nontoxic, and bioassimilibity.[61] Indeed, Kricheldorf et al. reported a series of manganese salts ($MnCl_2$, $MnBr_2$, and Mn(OAc)$_2$) as Lewis acid catalysts in the ROP of L-LA, though low activities were observed.[62,63] In a separate study, a new family of Salen–Manganese (III) complexes were investigated by Yang et al. as catalysts for the ROP of lactide in propylene oxide.[64] Most recently, Hu and coworker reported bimetallic manganese complexes as catalysts for ROP of enantiopure L-LA with moderate catalytic and better control of the polymerization reactions activities.[65]

Inspired by the promising nature of the use of manganese-based catalysts in these ROP reactions, were opted to explore the ROP of *rac*-lactides (*rac*-LA) using manganese complexes derived from Schiff-base (imino)pyridine/phenol proligands. The choice of these ligands was motivated by their ease of

M. Zikode, A. Ngwenya, S. O. Ojwach
School of Chemistry and Physics
University of KwaZulu-Natal
Pietermaritzburg Campus, Private Bag X01, Pietermaritzburg 3209, South Africa
E-mail: ojwach@ukzn.ac.za

T. Becker, S. Herres-Pawlis
Institute of Inorganic Chemistry
RWTH Aachen University
Landoltweg 1, 52074 Aachen, Germany

Supporting information for this article is available on the WWW under https://doi.org/10.1002/ejic.202500126

Research Article
doi.org/10.1002/ejic.202500126

synthesis, modification, and formation of highly stable metal complexes. Thus, we, herein, report the synthesis, structural elucidation, and applications of a new series of manganese catalysts supported by the (imino)pyridine/phenol proligands in the ROP of *rac*-LA. Detailed kinetics studies of the ROP reactions and polymer properties have been studied and will be discussed.

2. Results and Discussion

The (imino)phenol proligands (2[((2-hydroxyethyl)imino)methyl] phenol (**L1H$_2$**) and 2-[((2-methoxyethyl)imino)methyl]phenol (**L2H**)) were prepared following our recently reported protocols.[66] In contrast, the (imino)pyridine proligands ((E)-2-((pyridine-2-ylmethylene) amino) ethan-1-ol (**L3H**) and (E)-N-(2-methoxyethyl)-1-(pyridine-2-yl) methanimine (**L4**)) were prepared by the condensation of 2-pyridine carboxyaldehyde with the corresponding amine derivative (Scheme S1, Supporting Information). Treatment of (imino)phenol proligand (**L1H$_2$**) with $MnCl_2{\cdot}4H_2O$ afforded the tetranuclear Mn(III) complex [Mn(**L1**)Cl]$_4$ (**Mn1**) as shown in **Scheme 1**. The dianionic ligand (**L1**$^{2-}$) adopts a tridentate coordination mode to the Mn(II) central atom via the phenoxy, alkoxy oxygen, and nitrogen atoms as shown in Scheme 1 and **Figure 1**. The oxidation of Mn(II)–Mn(III) species have been reported in literature,[67–72] but in this case, may be attributed to the high acidity of both the phenoxy and alkoxy protons, leading to facile deprotonations. On the contrary, the reactions of $MnCl_2{\cdot}4H_2O$ with the ligand (**L2H**) afforded the respective mononuclear complex [Mn(**L2**)$_2$(CH$_3$OH)$_2$] (**Mn2**) (Scheme 1). Separately, the reactions of (imino)pyridine proligands (**L3H** or **L4**) with equimolar amounts of $MnCl_2{\cdot}4H_2O$ salt, afforded the polynuclear Mn(II) complexes [Mn(**L3H**)Cl$_2$]$_3$ (**Mn3**) and [Mn(**L4**)Cl$_2$]$_3$ (**Mn4**), respectively (Scheme 1). The complexes were obtained in low yields (32%–37%) and were soluble in most organic solvents, such as acetone, MeOH, EtOH, THF, acetonitrile, DMF, and DMSO.

The formation and identities of the ligands were established using nuclear magnetic resonance (NMR) and Fourier trasnform - infra red (FT-IR) spectroscopies (Figure S1–S12, Supporting Information). However, due to the paramagnetic nature of the manganese complexes, NMR spectroscopic characterization was not useful, hence, we employed FT-IR spectroscopy (Table S1 and Figure S13–S16, Supporting Information). In general,the FT-IR spectra of complexes **Mn1**–**Mn4** showed the imine ν(C═N) stretching frequencies at lower wavenumbers relative to the free ligands (Table S1, Supporting Information). For example, the ν(C═N) stretching frequency of complex **Mn3** and its ligand **L3H** were recorded at 1595 from 1649 cm^{-1}, respectively (Figure S15, Supporting Information), in good agreement with previous findings.[73–75] The O—H functionality was instrumental in the deduction of the nature of the coordination complexes formed. Notably, the signal corresponding to the ν(O—H) frequency at 3368 cm^{-1} in **L1H$_2$** (Figure S9, Supporting Information), was not observed in the corresponding complex **Mn1** (Figure S13, Supporting Information), consistent with the O—H deprotonation of the ligand prior to coordination as shown in Scheme 1. The signal observed at around 3441 cm^{-1} in complex **Mn2** (Figure S14, Supporting Information) could be assigned to the O—H group in the coordinated methanol solvent (Scheme 1). In contrast, complex **Mn3** recorded the ν(O—H) band at 3432 cm^{-1} relative to 3268 cm^{-1} in the free ligand **L3H** (Figure S11 and S15, Supporting Information), further supporting the absence of O—H deprotonation of **L3H** as shown in Scheme 1. Electron spray ionization mass spectrometry (ESI-MS) was also

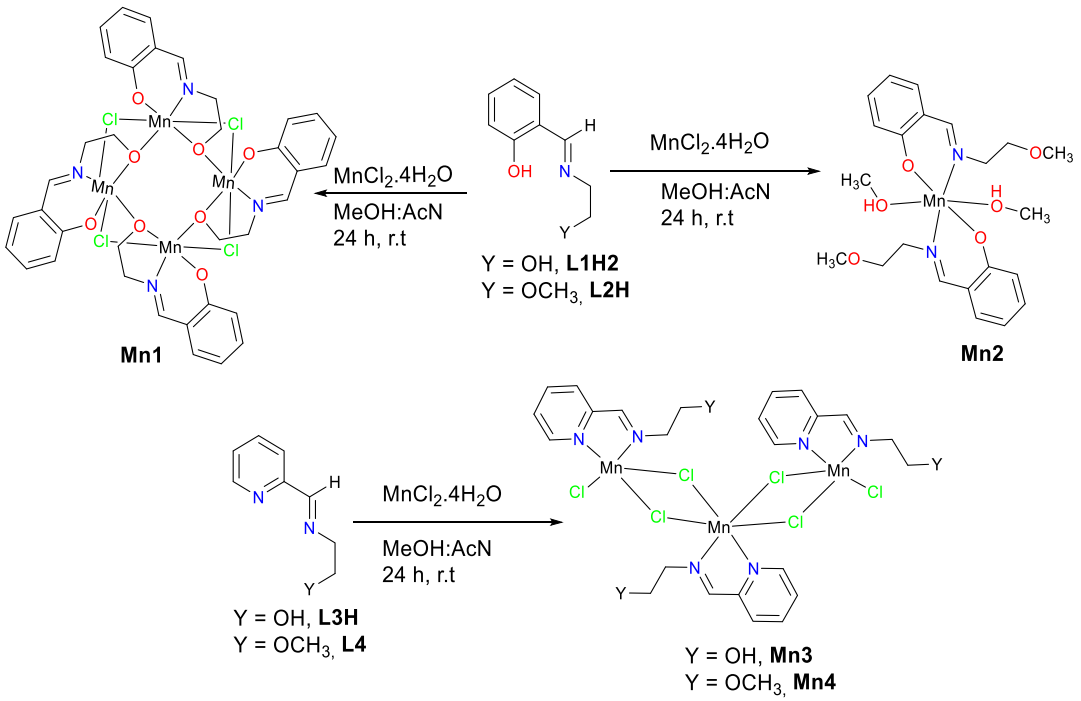

Scheme 1. Synthesis of Mn(II) and Mn(III) complexes (**Mn1**–**Mn4**) bearing (imino)phenol/pyridine proligands.

Research Article
doi.org/10.1002/ejic.202500126

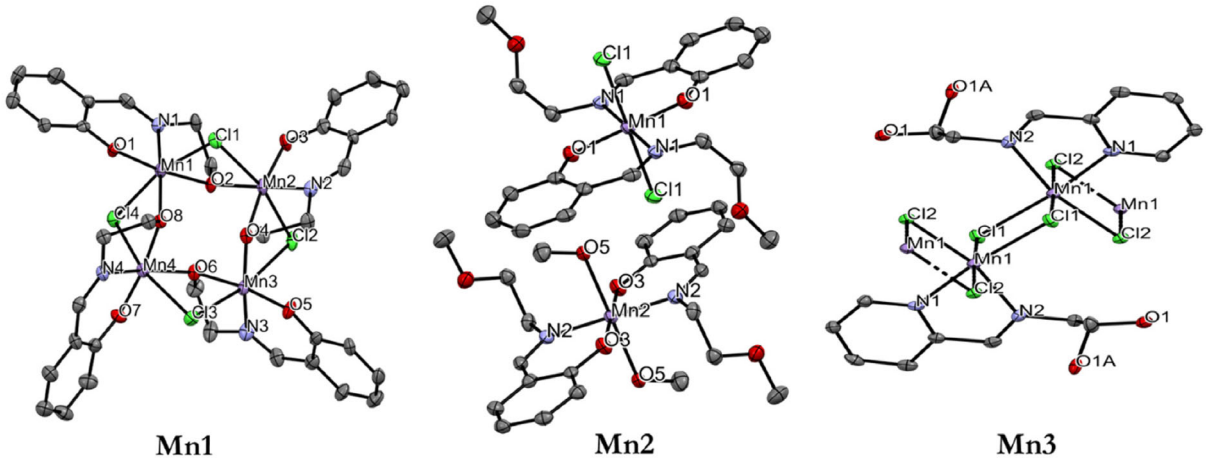

Figure 1. Molecular structures of Mn(II) and Mn(III) complexes **Mn1**, **Mn2,** and **Mn3** drawn with thermal ellipsoids drawn at 50% probability level, hydrogens are omitted for clarity.

used to determine the molecular compositions of complexes **Mn1**–**Mn4** (Figure S17–S20, Supporting Information). For instance, complexes **Mn1** and **Mn2** exhibited base peaks at $m/z = 296$ (**Mn1**) and $m/z = 411$ (**Mn2**) corresponding to the $[M - (MnL1)_3Cl_2), + Li]^+$ and $[M - (CH_3OH)_2]^+$ fragments, respectively (Table S1, Figure S17 and S18, Supporting Information). On the contrary, the ESI-MS spectra of complexes **Mn3** and **Mn4** were identified with the base respective peaks ($m/z = 479$ [**Mn3**] and $m/z = 254$ [**Mn4**]) corresponding to the $[M\text{-}(MnL4H)Cl_4]^+$ and $[M\text{-}(MnL5)_2Cl_5]^+$ fragments, respectively (Table S1, Figure S19 and S20, Supporting Information).

2.1. Molecular Structures of Compounds Mn1, Mn2 and Mn3

Molecular structures of compounds **Mn1**, **Mn2,** and **Mn3** were further elucidated using single crystal X-ray crystallography analyzes. Single crystals suitable for X-ray crystallography analyzes for compound **Mn1** were grown by layering methanol solution with acetone while slow evaporation of methanol/acetonitrile mother liquor afforded single crystals for compounds **Mn2** and **Mn3**. Crystal data collection and structural refinement parameters are presented in (Table S2, Supporting Information). The respective solid state structures and selected bond lengths and angles are given in Figure 1 and Table S3, Supporting Information, respectively. Both the tetranuclear complex **Mn1** and the cocrystal complex **Mn2** crystallized in the P-1 triclinic space groups. Boskovic and coworkers reported a similar structure to compound **Mn1,** though the data was collected at a higher temperature of 153 K, compared to the current data set, which were collected at 100 K.[71,72] Even though both compounds crystallize in the same space group, the current compound **Mn1** has an increased volume and a unit cell ($V = 2385.3(6)$ Å^3, $z = 4$) compared to the previously reported of $V = 1984.8(4)$ Å^3, $z = 2$, and is consistent with the presence of acetone solvent in the current complex **Mn1**. In compound **Mn1**, each Mn(III) metal center is hexa-coordinated, with one dianionic ligand ($L1^{2-}$) tridentately coordinated to the Mn(III) metal center through the phenoxo-oxygen, the imine-nitrogen, and the pendant-arm oxygen atoms. Two chlorido ligands and the pendant-arm oxygen atom of the second ligand bridges the two Mn(III) centers. In contrast, compound **Mn2** contains two cocrystals, which are both mononuclear, hexa-coordinated with two ligands bidentately coordinated to each Mn(II) metal center through the phenoxo-oxygen and imine-nitrogen atoms. Interestingly, while the ligands on the first cocrystal are neutral, balanced by two chloride ligands, the second cocrystal contains mono-anionic ($L3H^-$) ligands, with two methanol ligands completing the octahedral arrangement. In compound **Mn3**, each Mn(II) metal center exhibits hexa-coordination, where the coordination sphere consists of a bidentately coordinated N^N ligand (**L3H**) and four bridging chlorido ligands.

While the bond angles of 170.13(14)° for Cl—Mn1—Cl, and 177.01(3)° for O—Mn1—O for complexes **Mn1** and **Mn3,** respectively, depict distorted octahedral geometries, complex **Mn2** has a bond angle of 180.0° for O—Mn1—N, consistent with a near perfect octahedral geometry. This is supported by the average N—O distance of 2.783 Å and bite angle of 90.77(10)° observed in compound **Mn2**, and the average N_{py}—N_{im} distance of 2.709 Å and chelate bite angle of 73.83(10)° observed in compound **Mn3**. The distortions in compounds **Mn1** and **Mn3** could be a consequence of a ligand rigidity and the presence of bridging ligands.[73,74] The average Mn—N_{imine} and Mn—$O_{phenoxo}$ bond lengths of 1.980 ± 0.008 and 1.862 ± 0.004 Å, respectively, for compound **Mn1** are comparable to the average bond lengths in compound **Mn2** (Mn—$N_{imine} = 2.040 \pm 0.007$ and Mn—$O_{phenoxo} = 1.857 \pm 0.004$ Å). However, the average Mn—N_{imine} bond length of 2.250 ± 0.065 Å for compound **Mn3** is slightly longer compared to the average bond lengths in **Mn1** (1.980 ± 0.008) and **Mn2** (2.040 ± 0.007 Å). The shorter Mn—N_{imine} average bond lengths in compound **Mn2** could be ascribed to the presence of a low spin Mn(II) center.[76] In addition, the average Mn—Cl bond lengths of 2.604 ± 0.169 and 2.624 ± 0.035 Å for **Mn1** and **Mn3,** respectively, are comparable.

In comparison to previously reported complexes, the Mn—$N_{pyridine}$ and Mn—N_{imine} average bond lengths of 2.261 ± 0.018 and 2.250 ± 0.065 Å for compound **Mn3** are longer than the average bond length of 2.243 ± 0.120 and 2.185 ± 0.083 Å reported in 12 and 10 similar structures,

Research Article
doi.org/10.1002/ejic.202500126

respectively.[77] In contrast, Mn—N_{imine} average bond length of 1.980 ± 0.008 and 2.040 ± 0.007 Å for **Mn1** and **Mn2** are comparable to the average bond lengths of 1.979 ± 0.013 and 2.038±0.044 Å reported in 7 and 17 similar structures, respectively.[78] It is also interesting to note that the Mn—$O_{phenoxo}$ average bond lengths of 1.862 ± 0.004 and 1.857 ± 0.004 Å for **Mn1** and **Mn2** are shorter than the average bond lengths of 1.883 ± 0.024 and 2.040 ± 0.035 Å reported in 10 and 47 structures, respectively.[78] While the average bond length for Mn—Cl of 2.624 ± 0.035 Å in compound **Mn3** is slightly longer than the average bond length of 2.564 ± 0.061 Å, reported in 5 similar structures, the average bond length for Mn—Cl of 2.604 ± 0.169 Å in **Mn1** is slightly shorter than the average bond length of 2.639 ± 0.067 Å reported for 10 similar structures.[78]

2.2. Ring-Opening Polymerization (ROP) of *rac*-Lactide (*rac*-LA)

2.2.1. Kinetics of ROP Reactions of rac-LA Catalysed by Complexes Mn1–Mn4

The ability of the manganese complexes (**Mn1**–**Mn4**) to catalyze the ROP of *rac*-LA was studied under melt conditions (solvent-free) at 150 °C, monomer to metal ratio ([*rac*-LA]:[Mn]) of 100:1 using Schlenk tube techniques (**Scheme 2**). From the data collected in **Table 1**, all complexes showed moderate catalytic activities under these conditions. In general, the catalytic activities of the complexes was found to depend on both the ligand motif and the coordination chemistry. For example, while complexes **Mn1** and **Mn2** derived from N^O-donor (imino)phenol proligands

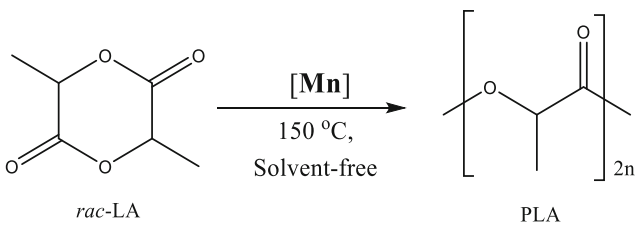

Scheme 2. The ROP of *rac*-LA using complexes **Mn1**–**Mn4** as initiator, [*rac*-LA]:[Mn] ratio of 100:1, 260 rpm, in bulk at 150 °C in the absence of an alcohol.

(**L1H$_2$** and **L2H**) afforded monomer conversions of up 92% within 2 h (Table 1, entries 1–2), the N^N-donor (imino)pyridine-based counterparts **Mn3**–**Mn4** reached monomer conversions up to 80% in 8 h (Table 1, entries 3–4).

To fully decipher the catalytic activities of complexes **Mn1**–**Mn4**, kinetic studies were performed by plotting ln([*rac*-LA]$_0$/[*rac*-LA]$_t$) vs time (**Figure 2**). Good linear fits were observed for all the complexes suggesting *pseudo*-first order kinetics with respect to the monomer. The apparent rate constants (k_{app}) were obtained from the slopes of linear curve in Figure 2 and given in Table 1. From the kinetics data, the tetranuclear complex **Mn1** exhibited the highest catalytic activity with k_{app} of 3.11×10^{-3} s^{-1} and turnover frequency (TOF) of 276 h^{-1} (Table 1, entry 1) compared to the other complexes; ($k_{app} = 1.40 \times 10^{-4}$ s^{-1}, TOF = 12.8 h^{-1} (**Mn2**), $k_{app} = 5.75 \times 10^{-5}$ s^{-1}, TOF = 10 h^{-1} (**Mn3**), and $k_{app} = 4.39 \times 10^{-5}$ s^{-1}, TOF = 7.9 h^{-1} (**Mn4**), and Table 1, entries 2–4, respectively). The higher catalytic activity of the Mn(III) **Mn1** complex is reasonable since Mn(III) complexes are generally known to be more active due to the greater electropositive metal Mn(III) atom.[79,80] In contrast, the d^5 electron configuration in Mn(II) center (complexes **Mn2**–**Mn4**) is more stable, resulting in less reactivity.[81] Furthermore, it also plausible to argue that the diminished catalytic activity of complex **Mn2** could be as a consequence of the coordinated methanol solvent, which is known to act as a chain transfer agent. Notably, comparable catalytic activities were observed for the (imino)pyridine complexes **Mn3** and **Mn4** (Table 1, entries 3–4), which is understandable due to their similar coordination chemistry. Interestingly, complex **Mn4** showed a short induction period (Figure S21, Supporting Information), which can be assigned to the possible precatalyst rearrangement, in this case, breaking of the polymeric chains. To the best of our knowledge, complex **Mn1** appears to be the most active manganese catalyst reported to date in the ROP of *rac*-LA under industrial relevant conditions.[62,63,65,82] For example, while the Mn(II) salts, (MnX_2, where X = Cl, Br, or Acetate) reported by Rajashekhar et al.[63] and Kricheldorf et al.,[62] achieved maximum conversions in days, the current catalyst **Mn1** reached maximum conversions in just 20 min. Under melt conditions at 130 °C, one of the most active Mn(III) catalyst based on diphenolate–diamino ligand[82] afforded 90% monomer conversion in 4 h using [*rac*-LA]:[Mn] ratios of 100:1, compared to 92% conversion afforded by **Mn1** in 20 min at 150 °C and [*rac*-LA]:[Mn] of 100:1 (Table 1, entry 1).

Table 1. Summary of *rac*-LA polymerization with manganese complexes **Mn1**–**Mn4**.

Entry[a]	Cat	Time [min]	Conv.[b] [%]	k_{app}[c] [s^{-1}]	TOF[d] [h^{-1}]	$M_{n,theo}$[e] [g mol^{-1}]	$M_{n,GPC}$[f] [g mol^{-1}]	$Đ$[g]	P_r[h]
1	**Mn1**	20	92	3.11×10^{-3}	276	13 260	5000	1.8	0.55
2	**Mn2**	360	77	1.40×10^{-4}	12.8	11 098	3800	1.4	0.58
3	**Mn3**	480	80	5.75×10^{-5}	10	11 530	6400	1.7	0.55
4	**Mn4**	480	63	4.39×10^{-5}	7.9	9080	n.d	n.d	0.59

[a]All polymerization reactions were carried out under molten state at 150 °C at [*rac*-LA]/[Mn] of 100:1, using nonpurified *rac*-LA. [b]Determined by ^{1}H NMR spectroscopy. [c]Determined from the slopes of the plots of ln([*rac*-LA]$_0$/[*rac*-LA]$_t$) versus time. [d]TOF = ([*rac*-LA]/[Mn] × conv.%)/(time(h)). [e]$M_{n,theo}$ = [*rac*-LA]/[Mn] × molar mass of *rac*-LA × conversion. [f]Determined by GPC in THF relative to polystyrene standards (correction factor = 0.58). [g]Determined by GPC obtained by M_w/M_n. [h]P_r is the probability of racemic linkages between monomer units, determined by homonuclear-decoupled ^{1}H NMR spectroscopy.

Research Article
doi.org/10.1002/ejic.202500126

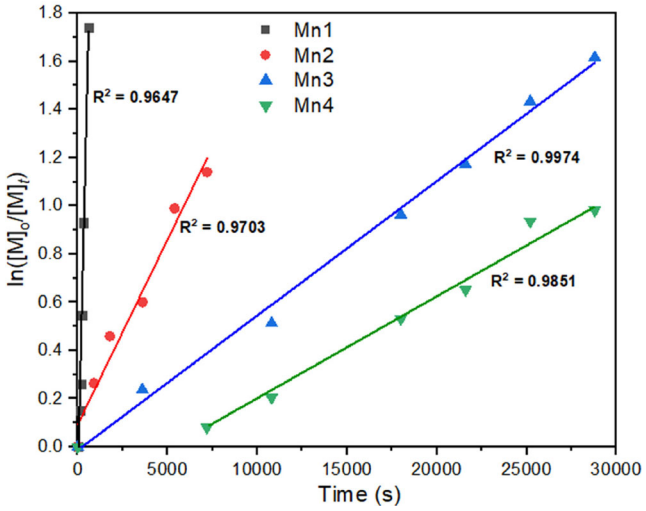

Figure 2. The semi-logarithmic plots of $\ln([LA]_0/[LA]_t)$ versus time of the ROP of *rac*-LA using complexes **Mn1**–**Mn4** at [*rac*-LA]:[Mn] of 100:1, solvent-free conditions at 150 °C, and 260 rpm using Schlenk tube techniques.

2.2.2. Effect of the Addition of Benzyl Alcohol

It is generally known that the addition of alcohol-initiators in the ROP of lactides could have profound effects on the catalytic performance of metal complexes, both in terms of activity and polymer properties. Initially, we investigated the catalytic activities of complexes **Mn1**–**Mn4** in the ROP of *rac*-LA in the absence of alcohol in air for direct comparisons with the reactions carried out using benzyl alcohol as a co-initiator (**Table 2**). The polymerization reactions were conducted at [*rac*-LA]:[Mn] of 100:1, solvent-free conditions at 150 °C (Table 2, entries 1–4). In general, all the complexes were slightly sensitive to the atmospheric conditions and achieved maximum conversions within 5–120 h. For example, the imino-phenol-based complexes, **Mn1**–**Mn2,** showed 16-fold (86%, TOF = 17.2 h^{-1}) and 18- fold (89%, TOF = 0.7 h^{-1}) lower catalytic activities in air (Table 2, entries 1–2) compared to the catalytic activities reported under inert environment of TOF = 276 and 12.8 h^{-1}, respectively (Table 1, entries 1–2). Notably, the imino-pyridine-based complexes **Mn3**−**Mn4** showed improved stability under atmospheric conditions, recording TOF = 3.3 and 3.6 h^{-1} in air (Table 2, entries 3–4) compared to the TOFs of 10 and 7.9 h^{-1} under inert environment, respectively (Table 1, entries 3–4).

Table 2. Summary of *rac*-LA polymerization with manganese complexes **Mn1**–**Mn4** performed in air.

Entry[a)]	Cat	[*rac*-LA]: [Mn]:[BnOH]	Time [h]	Conv.[b)] [%]	TOF[c)] [h^{-1}]
1	**Mn1**	100:1:0	5	86	17.2
2	**Mn2**	100:1:0	120	89	0.7
3	**Mn3**	100:1:0	24	79	3.3
4	**Mn4**	100:1:0	24	87	3.6
5	**Mn1**	100:1:1	4	>99	24.8
6	**Mn2**	100:1:1	48	80	1.7
7	**Mn3**	100:1:1	18	87	4.8
8	**Mn4**	100:1:1	22	91	4.1

[a)]All polymerization reactions were carried out under molten state at 150 °C at [*rac*-LA]:[Mn] :[BnOH], using nonpurified *rac*-LA. [b)]Determined by ^{1}H NMR spectroscopy. [c)]TOF = ([*rac*-LA]/[Mn]:[BnOH × conv.%)/(time[h]).

The polymerization reactions in the presence of benzyl alcohol as a co-initiator were performed at [*rac*-LA]:[Mn]:[BnOH] of 100:1:1 in a Schlenk tube at 150 °C (Table 2). Consistent with literature reports,[64,65,82] the presence of benzyl alcohol increased the polymerization rates of all the catalysts (Table 2, entries 5–8). In particular, complex **Mn1** showed the highest enhanced catalytic activity in the presence of benzyl alcohol. For example, using complex **Mn1**, >99% (TOF = 24.8 h^{-1}) monomer conversion was observed within 4 h in the presence of benzyl alcohol, compared to 86% (TOF = 17.2 h^{-1}) monomer conversion reported within 5 h in the absence of benzyl alcohol (Table 2, entries 1 and 5).

2.2.3. Determination of Propagation Rate Constant (k_p) of Complex Mn1

Further kinetic studies were performed using the most active complex **Mn1** in order to determine the rate constant of propagation (k_p).[65] The ROP reactions were thus carried out at varied [*rac*-LA]:[Mn] ratios of 100:1, 500:1, 750:1, 1000:1, and 1500:1. The apparent rate constants k_{app} were determined from the slopes of the semilogarithmic plot ($\ln([rac\text{-LA}]_0/[rac\text{-LA}]_t$) versus time for each catalyst concentration as shown in Figure S22, Supporting Information. The catalytic trends show that the k_{app} values decreased with an increase in catalyst loadings. For example, complex **Mn1** exhibited rate constants ($k_{app} = 6.89 \times 10^{-5}$ s^{-1}) nearly forty-five times lower at [*rac*-LA]:[Mn] ratio of 1500:1 compared to $k_{app} = 3.11 \times 10^{-3}$ s^{-1} at [*rac*-LA]:[Mn] ratio of 100:1. The propagation rate constant (k_p) was then determined from the slopes of the plot of apparent rate constants k_{app} at different catalyst concentrations vs time (**Figure 3**). A k_p value of $(4.25 \pm 0.15) \times 10^{-2}$ L mol^{-1} s^{-1} was obtained, and is slightly lower compared to the value of 0.167 L mol^{-1} s^{-1} reported for the commercial $Sn(Oct)_2$.[83]

2.2.4. Determination of Rate Order and Overall Rate Law of Polymerization Reactions

Further kinetics studies were performed in order to illuminate the order of the ROP reactions with respect to catalyst **Mn1** by plotting the graph of $-\ln k_{app}$ versus −ln[**Mn1**] as shown in Figure S23, Supporting Information. From Figure S23, Supporting Information, a fractional rate order of 1.32 with respect to catalyst **Mn1** concentration was obtained. Thus, combined with the first order kinetics with respect to monomer, the overall rate law can be represented as given in Equation (1). The fractional rate order with respect to [**Mn1**] could be ascribed to disintegration of the tetranuclear core, as supported by the fragmentation patterns observed in the mass spectrometry spectrum of complex **Mn1** (Figure S17, Supporting Information). To support this assertion, while no molecular ion peak at *m/z* = 1012 amu was recorded, the observed *m/z* signals at 724, 471, and 344 amu correspond

Research Article
doi.org/10.1002/ejic.202500126

Chemistry Europe
European Chemical Societies Publishing

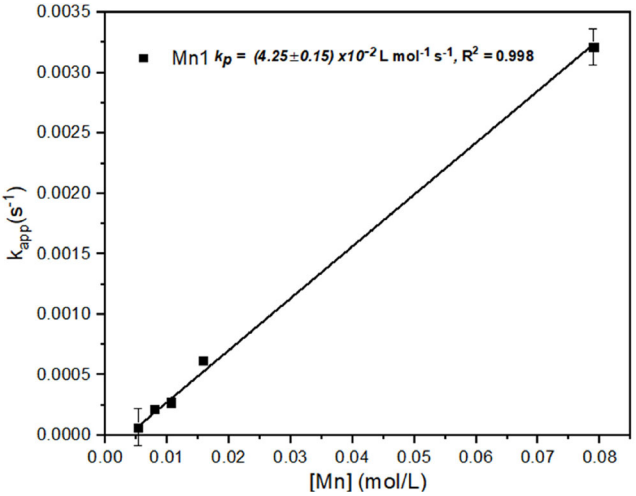

Figure 3. Linear plot of k_{app} versus [**Mn1**], the slope of the linear plot represents the propagation rate constant k_p value, which is $(4.25 \pm 0.15) \times 10^{-2}$ (**Mn1**, $R^2 = 0.998$) L mol^{-1} s^{-1}. Polymerization reaction conditions: nonpurified *rac*-LA; 150 °C; 260 rpm; solvent-free; and [*rac*–LA]/[Mn] = 100:1, 500:1, 750:1, 1000:1, and 1500:1 using Schlenk tube techniques.

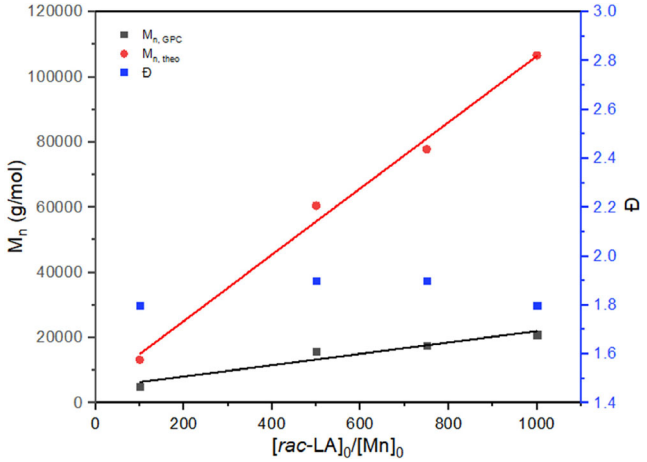

Figure 4. Plot of $M_{n,GPC}$ (g mol^{-1}), $M_{n,theo}$ (g mol^{-1}), and $Đ$ versus [*rac*-LA]$_0$/[Mn]$_0$ for ROP of *rac*-LA at 150 °C using complex **Mn1**.

to the trinuclear, dinuclear, and mononuclear species, respectively (Figure S17, Supporting Information). Thus, the fraction reaction order of 1.32 with regard to catalyst **Mn1** could originate from the presence of these different fragments as active species, consistent with previous literature reports.[84,85] In general, the order can be treated as first order kinetics as depicted in Equation (1) to give an overall of two.

$$Rate = -d[rac-LA]/dt = k_p[rac-LA]^1[\mathbf{Mn1}]^1 \quad (1)$$

2.2.5. Determination of Molecular Weights and Polymer Microstructure

To determine the polymer molecular weights and dispersities ($Đ$), gel permeation chromatography (GPC) using polystyrene standards was employed. Generally, low average number molecular weights (M_n up to 6 400 g mol^{-1}) and moderate dispersities ($Đ = 1.2$–1.8) at [*rac*-LA]:[**Mn**] ratio of 100:1 were recorded (Table 1, entries 1–4). Appreciable discrepancies between the observed average number molecular weights (GPC) and theoretical molecular weights were also evident. For an example, complex **Mn1** afforded polymers with experimental molecular weight of 5 000 g mol^{-1}, compared to the theoretical molecular weights of 13 260 g mol^{-1} (Table 1, entry 1 and **Figure 4**). The observed lower experimental molecular weights could be attributed to the presence of different catalyst fragments as discussed in Figure S17, Supporting Information. It is also possible to argue that high viscosity and the occurrence of side reactions, such as transesterification, could be a contributing factor.[86–88] Nonetheless, the linearity of the plots of M_n versus % conversions for complexes **Mn1** and **Mn2** and invariable $Đ$ values, partly indicated controlled polymerization reactions (Figure S24–25, Supporting Information). Unfortunately, the reactions performed under atmospheric conditions, both in the presence or absence of benzyl alcohol (Table 2), did not result in any pol(lactide) precipitates, depicting possible formation of very low molecular weight PLAs or oligomeric materials. Formation of low molecular weight polymers in the presence of alcohol initiators is associated with the presence of multiinitiating groups/different growing polymer chains.[89] To determine the polymer microstructure and tacticities, homonuclear decoupled ^{1}H{^{1}H} NMR spectra was utilized (Figure S26–29, Supporting Information). The complexes afforded mainly atactic biased polymers with $P_r = 0.58$–0.59 (Table 1, entries 1–4) showing no signs of any isoselectivity.

2.2.6. End Group Analysis and Mechanistic Pathways

In order to establish the nature of the end-groups of the polymers and the mechanism of the ROP reactions of the *rac*-LA using these complexes, a polymer sample (at 86% conversion) produced from catalyst **Mn1** at [*rac*-LA]$_0$/[**Mn1**]$_0$ molar ratio of 100:1 under melt conditions at 150 °C was analyzed using atmospheric pressure chemical ionization mass spectrometry (APCI-MS). The APCI mass spectrum in Figure S30, Supporting Information, is consistent with the polymer being end-capped by the ligand (**L1**) and —OH end-groups. For instance, the peak observed at 1247.3 g mol^{-1} in the APCI spectrum corresponds to $HOCHCH_3CO(OCHCH_3CO)_n$—$C_9H_{10}NO_2$, and consists of the terminated polymer with n($OCHCH_3CO$) ($n = 14$), the rest of the polymer chain ($145–(72)_n = 73$ amu), the ligand ($C_9H_{10}NO_2 = 164$ amu) as depicted in Figure S30, Supporting Information. It is worth mentioning that the repeating units are separated by 72 Da which points to the presence of transesterification reactions.[82,90–93] The results obtained suggest that the ROP of *rac*-LA follows the coordination-insertion mechanism, rather than activated monomer mechanism.[94]

3. Conclusions

In this contribution, we have reported a new family of rare manganese(II)/(III) complexes bearing (imino)phenol (**Mn1**–**Mn2**)

and (imino)pyridine proligands (**Mn3**–**Mn4**) as catalysts in the ROP of *rac*-LA. The (imino)pyridine proligands (**L3H** and **L4**) afforded polynuclear complexes, whereas, the (imino)phenol proligands (**L1H$_2$** and **L2H**) witnessed diverse coordination modes to give both mononuclear and tetranuclear complexes, depending on the nature of the pendant groups. The complexes exhibited high catalytic activities in the ROP of *rac*-LA under industrial and melt conditions, affording moderately dispersed atactic biased polymers with moderate molecular weights. Complexes, **Mn1** and **Mn2**, based on (imino)phenol proligands, exhibited higher activities when compared to the polynuclear (imino)pyridine-based complexes **Mn3** and **Mn4**. All complexes showed increased activities in the presence of benzyl alcohol as a co-initiator. The tetranuclear complex **Mn1** was the most active and to the best of our knowledge, the rate constant of $k_p = 4.25 \pm 0.15 \times 10^{-2}$ L mol^{-1} s^{-1} is the highest reported to date in literature for any manganese complex in the ROP of *rac*-lacitde under melt conditions. The polymerization reactions in the absence of benzyl follow coordination-insertion mechanism. Thus, this work has the potential to open new frontiers on the use of the naturally abundant and affordable manganese-based complexes as catalysts for the production of biodegradable polyesters.

4. Experimental Section

Synthesis of (Imino)Phenol/Pyridine Manganese Complexes: General Synthesis of Complexes Mn1–Mn4

To a stirred solution of $MnCl_2.4H_2O$ in a 1:1 v/v mixture of methanol/acetonitrile (20 mL), one equivalent of the corresponding ligand, was added dropwise and stirred for 24 h at room temperature. The crude products were filtered, washed with cold acetonitrile (2 × 10 mL), followed by diethyl ether (2 × 10 mL), and then, dried under vacuum to give the respective manganeses complexes.

Synthesis of (Imino)Phenol/Pyridine Manganese Complexes: [Mn(L1)Cl]$_4$ (Mn1)

2-[((2-hydroxyethyl)imino)methyl]phenol (**L1H$_2$**) (0.20 g, 1.21 mmol) and $MnCl_2.4H_2O$ (0.24 g, 1.21 mmol) afforded a brownish solid. Single crystals suitable for X-ray analysis were grown by layering diethyl ether on methanol solution. Yield = 0.45 g (37%). FT-IR (cm^{-1}): (ν_{C-H})$_{alkyl}$ 2930, ($\nu_{C=Nimine}$) 1625, and (ν_{C-O}) 1294. ESI-MS: *m/z* (%) 296 [(M^+ − (MnL1)$_3$Cl$_2$, + Li + 2 H$^+$, 100%). Anal. Calc. for $C_{36}H_{36}Cl_4Mn_4N_4O_8$ C, 42.63; H, 3.58; and N, 5.52. Found: C, 42.68; H, 3.36; and N, 5.58.

Synthesis of (Imino)Phenol/Pyridine Manganese Complexes: [Mn(L2)$_2$(CH$_3$OH)$_2$] (Mn2)

2-[((2-methoxyethyl)imino)methyl]phenol (**L2H**) (0.20 g, 1.12 mmol) and $MnCl_2.4H_2O$ (0.20 g, 1.12 mmol) afforded a green solid. Single crystals suitable for X-ray analysis were grown by slow evaporation in MeOH/Acetonitrile solution. Yield = 0.18 g (34%). FT-IR (cm^{-1}): (ν_{N-H}) 3317, (ν_{C-H})$_{alkyl}$ 2916, ($\nu_{C=Nimine}$) 1619, (ν_{N-H}) 1468, and ($\nu_{C-Oether}$) 1153. ESI-MS: *m/z* (%) 411 [(M^+ – (MnL1H)Cl$_4$, 100%). Anal. Calc. for $C_{22}H_{32}MnN_2O_6.2MeOH$: C, 48.56; H, 5.30; and N, 5.66. Found: C, 48.24; H, 4.96; and N, 5.42.

Synthesis of (Imino)Phenol/Pyridine Manganese Complexes: [Mn(L3H)Cl$_2$]$_3$ (Mn3)

(E)-2-((pyridine-2-ylmethylene)amino)ethan-1-ol (**L3H**) (0.33 g, 2.18 mmol) and $MnCl_2.4H_2O$ (0.43 g, 2.18 mmol) afforded a yellow solid. Single crystals suitable for X-ray analysis were grown by slow evaporation in MeOH/Acetonitrile solution. Yield = 0.58 g (32%). FT-IR (cm^{-1}): (ν_{H-O})$_{alkoxo\text{-}hydroyl}$ 3402, (ν_{C-H})$_{alkyl}$ 2960, ($\nu_{C=N}$)$_{imine}$ 1645, (ν_{C-O}) 1283, and (ν_{O-H})$_1$°$_{alcohol}$ 1030. ESI-MS: *m/z* (%) 479 [(M^+ – (MnL4H)Cl$_4$, 100%). Anal. Calc. for $C_{24}H_{30}Cl_6Mn_3N_6O_3$: C, 34.81; H, 3.65; and N, 10.15. Found: C, 34.50; H, 3.65; and N, 10.08.

Synthesis of (Imino)Phenol/Pyridine Manganese Complexes: [Mn(L4)Cl$_2$]$_3$ (Mn4)

(E)-N-(2-methoxyethyl)-1-(pyrid-2-yl)methanimine (**L4**) (0.36 g, 2.18 mmol) and $MnCl_2.4H_2O$ (0.43 g, 2.18 mmol) afforded a cream-white solid. Yield = 0.67 g (35%). FT-IR (cm^{-1}): (ν_{C-H}), 2943, ($\nu_{C=Nimine}$); 1621, and (ν_{C-O}), 1153. ESI-MS: *m/z* (%) 254 [(M^+ – (MnL5)$_2$Cl$_5$, 100%). Anal. Calc. for $C_{27}H_{36}Cl_6Mn_3N_6O_3$: C, 37.27; H, 4.17; and N, 9.66. Found: C, 37.21; H, 3.91; and N, 9.49.

Deposition Numbers https://www.ccdc.cam.ac.UK/services/structures?id=doi:10.1002/###.20220XXX" –2 423 017 - 2 423 019 for complexes **Mn1–Mn3**, contain the supplementary crystallographic data for this paper. These data are provided free of charge by the joint Cambridge Crystallographic Data Centre http://www.ccdc.cam.ac.UK/structures Access Structures service. The spectroscopic data, detailed experimental procedures, tables and figures associated with this article are available free of charge in ESI (electronic supplementary information).

Acknowledgements

The authors are grateful for the financial support received from the AROP–RWTH Aachen, NRF-South Africa-ERTTG (151521) and NRF-South-CPRR (SRUG200408511611) for financial support. The scientific activities of the Bioeconomy Science Center were financially supported by the Ministry of Culture and Science within the framework of the NRW Strategieprojekt BioSC BioPlastiCycle (grant no. 313/323–400-00213).

Conflict of Interest

The authors declare no conflict of interest.

Author Contributions

Mnqobi Zikode: conceptualization, methodology, software, validation and editing, and writing—original draft preparation; **Asanda Ngwenya**: methodology and validation; **Tabea Becker**: validation and editing of final draft; **Sonja Herres-Pawlis**: supervision and writing—review and editing; **Stephen O. Ojwach**: conceptualization, writing—review and editing, supervision, and funding. All authors have read and agreed to the published version of the manuscript.

Data Availability Statement

The data that support the findings of this study are available in the supplementary material of this article.

Keywords: kinetics · lactides · manganese · polymerization · structures

[1] L. Lebreton, A. Andrady, *Palgrave Commun.* **2019**, *5*, 6.
[2] E. MacArthur, *Science* **2017**, *358*, 843.
[3] a) R. Geyer, J. R. Jambeck, K. L. Law, *Sci. Adv.* **2017**, *3*, e1700782; b) Plastics Europe **2021**, pp. 1–34. c) R. C. Hale, B. Song, *Environ. Sci. Technol.* **2020**, *54*, 7034; d) N. Parashar, S. Hait, *Sci. Total Environ.* **2021**, *759*, 144274.
[4] F. Santulli, G. Gravina, M. Lamberti, C. Tedesco, M. Mazzeo, *Mol. Catal.* **2022**, *52B*, 112480.
[5] A. Arbaoui, C. Redshaw, *Polym. Chem.* **2010**, *1*, 801.
[6] A. Corma, S. Iborra, A. Velty, *Chem. Rev.* **2007**, *107*, 2411.
[7] J. W. Rhim, H. M. Park, C. S. Ha, *Prog. Polym. Sci.* **2013**, *38*, 1629.
[8] G. Q. Chen, M. K. Patel, *Chem. Rev.* **2012**, *112*, 2082.
[9] N. F. Zaaba, M. Jaafar, *Polym. Eng. Sci.* **2020**, *60*, 2061.
[10] K. M. Nampoothiri, N. R. Nair, R. P. John, *Bioresour. Technol.* **2010**, *101*, 8493.
[11] S. Farah, D. G. Anderson, R. Langer, *Adv. Drug Delivery Rev.* **2016**, *107*, 367.
[12] Y.-L. Wu, H. Wang, Y.-K. Qiu, X. J. Loh, *RSC Adv.* **2016**, *6*, 44506.
[13] A. Kramschuster, L. Turng, *J. Biomed. Mater. Res. Part B: Appl. Biomater.* **2010**, *92*, 366.
[14] P. Saini, M. Arora, M. N. V. R. Kumar, *Adv. Drug Delivery Rev.* **2016**, *107*, 47.
[15] M. Santoro, S. R. Shah, J. L. Walker, A. G. Mikos, *Adv. Drug Delivery Rev.* **2016**, *107*, 206.
[16] S. Yıldız, B. Karaagaç, G. Ozkoc, *Polym. Eng. Sci.* **2014**, *54*, 2029.
[17] R. P. Pawar, S. U. Tekale, S. U. Shisodia, J. T. Totre, A. J. Domb, *Recent Pat. Regener. Med.* **2014**, *4*, 40.
[18] A. J. R. Lasprilla, G. A. R. Martinez, B. H. Lunelli, A. L. Jardini, R. M. Filho, *Biotechnol. Adv.* **2012**, *30*, 321.
[19] M. S. Singhvi, S. S. Zinjarde, D. V. Gokhale, *J. Appl. Microbiol.* **2019**, *127*, 1612.
[20] M. A. Ghalia, Y. Dahman, *J. Polym. Res.* **2017**, *24*, 74.
[21] S. Mallick, Z. Ahmad, F. Touati, J. Bhadra, R. A. Shakoor, N. J. Al-Thani, *Ceram. Int.* **2018**, *44*, 16507.
[22] O. Avinc, A. Khoddami, *Fibre Chem.* **2009**, *41*, 391.
[23] J. Lunt, A. Shafer, *J. Ind. Text.* **2000**, *29*, 191.
[24] W. Wu, W. Wang, J. Li, *Prog. Polym. Sci.* **2015**, *46*, 55.
[25] E. Lih, S. Oh, Y. K. Joung, J. H. Lee, D. K. Han, *Prog. Polym. Sci.* **2015**, *44*, 28.
[26] M. Nofar, C. B. Park, *Prog. Polym. Sci.* **2014**, *39*, 1721.
[27] I. Armentano, N. Bitinis, E. Forutunati, S. Mattioli, N. Rescignano, R. Verdejo, M. A. Lopez-Manchado, J. M. Kenny, *Prog. Polym. Sci.* **2013**, *38*, 1720.
[28] R. Herrero-Vanrell, M. F. Refojo, *Adv. Drug Delivery Rev.* **2001**, *52*, 5.
[29] N. Peelman, P. Ragaert, B. De Meulenaer, D. Adons, R. Peeters, L. Cardon, F. Van Impe, F. Devlieghere, *Trend Food Sci. Technol.* **2013**, *32*, 128.
[30] a) A. C. Stanford, A. P. Dove, *Chem. Soc. Rev.* **2010**, *39*, 486; b) A. P. Dove, *Chem. Commun.* **2008**, *48*, 6446; c) O. Dechy-Cabaret, B. Martin-Vaca, D. Bourissou, *Chem. Rev.* **2004**, *104*, 6147; d) M. H. Chisholm, Z. J. Zhou, *Mater. Chem.* **2004**, *14*, 3081; e) R. E. Drumright, P. R. Gruber, D. E. Henton, *Adv. Mater.* **2000**, *12*, 1814; f) M. G. Cushion, P. Mountford, *Chem. Commun.* **2011**, *47*, 2276; g) Y. Sarazin, R. H. Howard, D. L. Hughes, S. M. Humphrey, M. Bochmann, *Dalton Trans.* **2006**, 340.
[31] P. Mckeon, M. D. Jones, *Sustainable Chem.* **2020**, *1*, 1.
[32] J. Payne, P. McKeown, M. D. Jones, *Polym. Degrad. Stab.* **2019**, *165*, 170.
[33] M. Hong, E. X.-Y. Chen, *Green Chem.* **2017**, *19*, 3692.
[34] J. J. Bozell, G. R. Petersen, *Green Chem.* **2010**, *12*, 539.
[35] Y. Fan, C. Zhou, X. Zhu, *Catal. Rev. Sci. Eng.* **2009**, *51*, 293.
[36] M. Dusselier, P. V. Wouwe, A. Dewaele, E. Makshina, B. F. Sels, *Energy Environ. Sci.* **2013**, *6*, 1415.
[37] C. S. M. Pereira, V. M. T. M. Silva, A. E. Rodrigues, *Green Chem.* **2011**, *13*, 2658.
[38] S. Aparicio, R. Alcalde, *Green Chem.* **2009**, *11*, 65.
[39] M. K. Kiesewetter, E. J. Shin, J. L. Hendrick, R. M. Waymouth, *Macromolecules* **2010**, *43*, 2093.
[40] P. V. S. Nylund, B. Monney, C. Weder, M. Albrecht, *Catal. Sci. Technol.* **2022**, *12*, 996.
[41] U. Herber, K. Hegner, D. Wolters, R. Siris, K. Wrobel, A. Hoffmann, C. Lochenie, B. Weber, D. Kuckling, S. Herres-Pawlis, *Eur. J. Inorg. Chem.* **2017**, *2017*, 1341.
[42] R. D. Rittinghaus, P. M. Schafer, P. Albrecht, C. Conrads, A. Hoffmann, A. N. Ksiazkiewicz, O. Bienemann, A. Pich, S. Herres-Pawlis, *ChemSuSchem* **2019**, *12*, 2161.
[43] J. Stewart, M. Fuchs, J. Payne, O. Driscoll, G. Kociok-Kohn, B. D. Ward, S. Herres-Pawlis, M. D. Jones, *RSC Adv.* **2022**, *12*, 1416.
[44] S. D'Aniello, S. Lavieville, F. Santulli, M. Simon, M. Sellitto, C. Tedesco, *Catal. Sci. Technol.* **2022**, *12*, 6142.
[45] F. Santulli, D. Pappalardo, M. Lamberti, A. Amendola, C. Barba, A. Sessa, G. Tepedino, M. Mazzeo, *ACS Sustainable Chem. Eng.* **2023**, *11*, 15699.
[46] S. Roy, S. Sarkar, P. K. S. Antharjanam, D. Chakraborty, *New J. Chem.* **2023**, *47*, 635.
[47] C. Di Iulio, M. Middleton, G. Kociok-Köhn, M. D. Jones, A. L. Johnson, *Eur. J. Inorg. Chem.* **2013**, *2013*, 1541.
[48] Y. Huang, W. C. Hung, M. Y. Liao, T. E. Tsai, Y. L. Peng, C. C. Lin, *J. Polym. Sci., Part A: Polym. Chem.* **2009**, *47*, 2318.
[49] N. M. Rezayee, K. A. Gerling, A. L. Rheingold, J. M. Fritsch, *Dalton Trans.* **2013**, *42*, 5573.
[50] Y. Huang, X. Kou, Y. L. Duan, F. F. Ding, Y. F. Yin, W. Wang, Y. Yang, *Dalton Trans.* **2018**, *47*, 8121.
[51] H. Wang, Y. Yang, H. Ma, *Inorg. Chem.* **2016**, *55*, 7356.
[52] Y. Yang, H. Wang, H. Ma, *Inorg. Chem.* **2015**, *54*, 5839.
[53] C. Romain, C. K. Williams, *Angew. Chem., Int. Ed.* **2014**, *53*, 1607.
[54] N. Ferrentino, F. Franco, F. Grisi, S. Pragiola, M. Mazzeo, C. Costabile, *Mol. Catal.* **2022**, *533*, 112799.
[55] D. Wannipurage, T. S. Hollingsworth, F. Santulli, M. Cozzolino, M. Lamberti, S. Groysman, M. Mazzeo, *Dalton Trans.* **2020**, *49*, 2715.
[56] C. A. Wheaton, P. G. Hayes, B. J. Ireland, *Dalton Trans.* **2009**, *25*, 4832.
[57] Z. Zheng, G. Zhao, R. Fablet, M. Bouyahyi, C. M. Thomas, T. Roisnel, O. Casagrande, J. F. Carpentier, *New J. Chem.* **2008**, *32*, 279.
[58] I. D'Auria, C. Tedesco, M. Mazzeo, C. Pellecchia, *Dalton Trans.* **2017**, *46*, 12217.
[59] M. G. Davidson, M. D. Jones, D. Meng, C. T. O'Hara, *Main Group Chem.* **2006**, *5*, 3.
[60] T. Rosen, I. Goldberg, W. Navarra, V. Venditto, M. Kol, *Angew. Chem. Int. Ed.* **2018**, *57*, 7191.
[61] C. E. Casey, M. C. Neville, K. M. Hambidge, *Am. J. Clin. Nutri.* **1989**, *49*, 773.
[62] H. R. Kricheldorf, D.-O. Damrau, *J. Macromol. Sci. A* **1998**, *35*, 1875.
[63] B. Rajashekhar, D. Chakraborty, *Polym. Bull.* **2014**, *71*, 2185.
[64] Z. Yang, C. Hu, R. Duan, Z. Sun, H. Zhang, X. Pang, L. Li, *Asian J. Org.* **2019**, *8*, 376.
[65] B. Li, C. Hu, Z. Yang, X. Pang, X. Chen, *Chem. Eur. J.* **2024**, *30*, e202302884.
[66] M. Zikode, M. Fuchs, T. Langletz, B. Lisa, S. Herres-Pawlis, S. O. Ojwach, *ChemCatChem* **2024**, *17*, e202400771.
[67] J. Yoo, A. Yamaguchi, M. Nakano, J. Krzystek, W. E. Streib, L.-C. Brunel, H. Ishimoto, G. Christou, D. N. Hendrickson, *Inorg. Chem.* **2001**, *40*, 4604.
[68] G. L. Abbati, A. Cornia, A. C. Fabretti, A. Caneschi, D. Gatteschi, *Inorg. Chem.* **1998**, *37*, 1430.
[69] G. L. Abbati, A. Cornia, A. C. Fabretti, A. Caneschi, D. Gatteschi, *Inorg. Chem.* **1998**, *37*, 3759.
[70] G. Aromı´, A. Bell, S. J. Teat, A. G. Whittaker, R. E. P. Winpenny, *Chem. Commun.* **2002**, *17*, 1896.
[71] C. Boskovic, R. Bircher, P. L. W. Tregenna-Piggott, H. U. Gudel, C. Paulsen, W. Wernsdorfer, A.-L. Barra, E. Khatsko, A. Neels, H. Stoeckli-Evans, *J. Am. Chem. Soc.* **2003**, *125*, 14046.
[72] C. Boskovic, E. Rusanov, H. Stoeckli-Evans, H. U. Gudel, *Inorg. Chem. Commun.* **2002**, *5*, 881.
[73] R. N. Egekenze, Y. Guitneh, R. Butcher, *Inorg. Chim. Acta* **2018**, *478*, 232.
[74] K. Ghosh, N. Tyagi, P. Kumar, U. P. Singh, N. Goel, *J. Inorg. Biochem.* **2010**, *104*, 9.
[75] R. A. Geiger, G. B. Wijeratne, V. W. Day, T. A. Jackson, *Eur. J. Inorg. Chem.* **2012**, *2012*, 1598.
[76] M. P. Jensen, M. L. McKee, *Inorg. Chem.* **1995**, *34*, 3319.
[77] I. J. Bruno, J. C. Cole, P. R. Edgington, M. Kessler, C. F. Macrae, P. McCabe, J. Pearson, R. Taylor, *Acta Crystallogr., Sect. B: Struct. Sci.* **2002**, *58*, 389.
[78] I. J. Bruno, J. C. Cole, P. R. Edgington, M. Kessler, C. F. Macrae, P. McCabe, J. Pearson, R. Taylor, I. R. Cooper, S. E. Harris, A. G. Orpen, *J. Chem. Inf. Comput. Sci.* **2004**, *44*, 2133.
[79] S. S. Eaton, G. R. Eaton, *Biochem. Biophys. Res. Commun.* **2011**, *416*, 1.
[80] C. Sarma, P. K. Chaurasia, S. L. Bharati, *Russ. J. Gen. Chem.* **2019**, *89*, 517.
[81] S. M. Graham, D. A. Baker, *J. Am. Chem. Soc.* **2002**, *124*, 4342.
[82] P. Daneshmand, F. Schaper, *Dalton Trans.* **2015**, *44*, 20449.
[83] P. M. Schäfer, P. Mckeown, M. Fuchs, R. D. Rittinghaus, A. Herrmann, J. Henkel, S. Seidel, C. Roitzheim, A. N. Ksiazkiewicz, A. Hoffmann, A. Pich, M. D. Jones, S. Herres-Pawlis, *Dalton Trans.* **2019**, *48*, 6071.
[84] B. M. Chamberlain, M. Cheng, D. R. Moore, T. M. Ovitt, E. B. Lobkovsky, G. W. Coates, *J. Am. Chem. Soc.* **2001**, *123*, 3229.

[85] C. K. Williams, L. E. Breyfogle, S. K. Choi, W. Nam, V. G. Young, Jr., M. A. Hillmyer, W. B. Tolman, *J. Am. Chem. Soc.* **2003**, *125*, 11350.
[86] F. Santulli, I. D'Auria, L. Boggioni, S. Losio, M. Proverbio, C. Costabile, M. Mazzeo, *Organometallics* **2020**, *39*, 1213.
[87] Y. Yu, G. Storti, M. Morbidelli, *Ind. Eng. Chem. Res.* **2011**, *50*, 7927.
[88] A. Hermann, T. Becker, M. A. Schäfer, A. Hoffmann, S. Herres-Pawlis, *ChemSusChem* **2022**, *15*, e202201075.
[89] R. Itzinger, C. Schwarzinger, C. Paulik, *J. Polym. Res.* **2020**, *27*, 383.
[90] M. Hu, X. Song, F. Wang, W. Zhang, W. Ma, F. Han, *New J. Chem.* **2022**, *46*, 1175.
[91] Z. R. Turner, J.-C. Buffet, D. O'Hare, *Organometallics* **2014**, *33*, 3891.
[92] X. Tang, M. Hong, L. Falivene, L. Caporaso, L. Cavallo, E. Y. X. Chen, *J. Am. Chem. Soc.* **2016**, *138*, 14326.
[93] S. K. Roymuhury, M. Mandal, D. Chakraborty, V. Ramkumar, *Polym. Chem.* **2021**, *12*, 3953.
[94] O. Dechy-Cabaret, B. Martin-Vaca, D. Bourissou, *Chem. Rev.* **2004**, *104*, 6147.

Manuscript received: March 10, 2025
Revised manuscript received: May 21, 2025
Version of record online: June 16, 2025